

EVALUATION OF DRAW SOLUTIONS FOR FORWARD OSMOSIS USING A SODIUM ALGINATE-BACTERIAL CELLULOSE MEMBRANE FOR WATER RECOVERY

Alyssa Mae Acyatan^a, Czarielle Audrey Lim^a, Aileen Orbecido^{a,b}, Liza Patacsil^c, Arnel Beltran^{a,b*}

^aChemical Engineering Department, De La Salle University, 2401 Taft Avenue Manila 1004 Philippines

^bCenter for Engineering Sustainable and Development Research, De La Salle University, 2401 Taft Avenue Manila 1004 Philippines

^cDepartment of Engineering Science, College of Engineering and Agro-Industrial Technology, University of the Philippines Los Baños, College, Los Baños, Laguna 4031 Philippines

Article history

Received

24 March 2021

Received in revised form

26 July 2021

Accepted

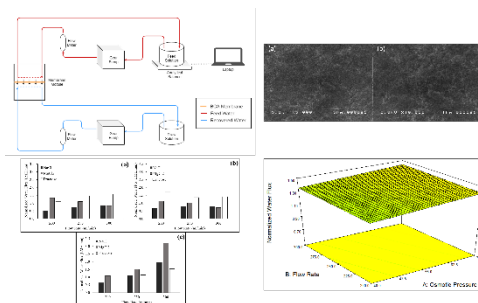
01 January 2022

Published online

31 May 2022

*Corresponding author
arnel.beltran@dlsu.edu.ph

Graphical abstract



Abstract

Forward osmosis (FO) is an emerging membrane technology that is comparable with existing industrial membrane separation processes. Several studies have shown the potential of bacterial cellulose-alginate (BCA) as membrane material for FO system. An ideal draw solution (DS) compatible with this material was investigated. The three solutions used in the study include NaCl, MgCl₂, and fructose. A simulated dirty water was used as the feed solution (FS) and a BCA as the membrane. An optimization study was conducted using central composite design (CCD) with the aid of Design Expert 7.0.0. The optimization was based on a fitted linear model analyzed through ANOVA with the normalized water flux maximized. The optimal solution was determined to be fructose with operating conditions at an osmotic pressure of 70 bar and a flow rate of 300 mL/min. The normalized water flux given these optimal conditions is predicted to be 1.437 LMH-mm with a desirability of 0.768.

Keywords: Bacterial cellulose, Draw solution, Forward osmosis, Sodium alginate, Water recovery

© 2022 Penerbit UTM Press. All rights reserved

1.0 INTRODUCTION

The Philippines continues to face several problems relating to water security due to its population increase, severe water pollution, and poor management over the years [1]. In a report by the Asian Development Bank, only 10% of the wastewater being discharged into bodies of water is being treated in the country [2]. Other countries in Asia and the Pacific also suffer from inadequate supply of clean water with 1.5 billion people living in rural areas and 0.6 billion in urban areas being affected [3]. With this demand for access to clean water, advances on wastewater technology have increased with membrane technology being one of the most important technologies in water treatment [4-5]. Majority have already been implemented in industries and the current filtration system being employed is reverse osmosis (RO). However, problems have risen from its

usage due to its high energy requirement which is related to its nature as a pressure-driven filtration process [6]. Further research on water recovery and treatment has led to investigating forward osmosis (FO) which has shown potential in resolving the issues noted from reverse osmosis [5].

In FO, the osmotic pressure difference between the FS and DS serves as the driving force for water to transport across a semi-permeable membrane. The process takes advantage of the properties of the FS and DS, thus it is often considered to be less energy intensive which translates to lower costs in operation depending on the desired output. The process, however, would require an additional step if it were to produce pure water which makes it less desirable compared to other membrane separation processes [6-7].

Many studies have been conducted on the fabrication of FO membranes. This was brought about by earlier studies that utilized membranes constructed for RO which are not suitable

for the FO process due to their dense nature and thickness [8]. One study focused on fabricating a composite FO membrane by modifying bacterial cellulose (BC) with sodium alginate (BCA) [9]. BC as a membrane has been used in several applications in the medical field and food industry [10]. There are recent studies that also utilized BC in separation processes, specifically for forward osmosis and desalination [9, 11-12]. However, studies on the selection of DS and operating parameters suitable for a BC membrane are still relatively few and have yet to be further investigated.

Selection of suitable DS is one major factor that greatly affects the water flux through the membrane and the cost-effectiveness of the FO process. The main conditions for choosing a suitable DS include capability to produce high osmotic pressure, high availability, non-toxicity, and low-cost recovery [13-14]. Commonly used DS are inorganic salts and simple sugars wherein both compounds account for 20% of the total publications in Scopus for FO from the year 1999 to 2020 [5]. Sodium chloride (NaCl) has become commonly used because of its high-water flux, low reverse solute flux, and low cost [15-17]. In addition, other inorganic solutes such as multivalent salts, magnesium chloride ($MgCl_2$), and magnesium sulfate ($MgSO_4$) have significant advantages over monovalent salts due to their larger molecular size that reduce reverse solute fluxes [13, 16, 18-19], and their ability to achieve higher osmotic pressures at the same molar concentrations. However, most multivalent salts cause high fouling on FO membranes and are costly to recover. This is where simple organics such as glucose [20], fructose [21], and sucrose [11] present an advantage as they are non-toxic and known to generate high osmotic pressure with minimal effect of reverse solute flux due to their large molecule size.

There is a need for an extensive analysis of DS that would best compliment the BCA membrane to enhance its performance in FO for water recovery. In this study, three different DS namely, NaCl, $MgCl_2$, and fructose, were tested to obtain their water flux at varying operating conditions. The operating parameters were set to osmotic pressures at 40, 55, and 70 bar and flow rates at 200, 250, and 300 mL/min. Experimental runs as well as optimization of these operating parameters were conducted following face-centered central composite design (CCD).

2.0 METHODOLOGY

Materials

The *Acetobacter xylinum* stock culture used in producing BC was purchased from the Department of Science and Technology - Advanced Science and Technology Institute (DOST-ASTI) in the Philippines. As for the DS, sodium chloride, magnesium chloride hexahydrate, and D-fructose were obtained from Loba Chemie Pvt. Ltd. (India). Calcium chloride dihydrate utilized for the simulated feed water was also from Loba Chemie. The soil was obtained from a local area in Makati, Philippines. The ammonium sulfate was obtained from HiMedia Laboratory Pvt. Ltd. (India). Glacial acetic acid (technical grade) was supplied from Merck (Germany) and sucrose from Techno Pharchem Haryana (India). The coconut water used for the culture medium was purchased in a local market in Manila, Philippines.

Fabrication of Bacterial Cellulose-Alginate Membrane

The composition of the culture medium used for the fabrication of the BC membrane is the same composition used in the studies conducted by Dang et al. and Suratago et al. [9, 22]. The culture medium was sterilized at 121 °C for 20 minutes before transfer. Pre-culture was prepared by adding 10 mL of *A. xylinum* mother liquor to 200 mL of culture medium.

For the BC membrane formation, 4 mL of the *A. xylinum* pre-culture was added to each petri dish containing 40 mL of culture medium. For 7 days, the inoculated culture medium was incubated using a Mytemp™ H2200 digital incubator at 30 ± 2 °C under static conditions. After 7 days of incubation, the formed membranes were placed under running water then treated with 0.2 N NaOH for 2 to 3 days until the membranes were stripped off of their excess proteins and have turned into a clear white color. After NaOH treatment, the membranes were washed with deionized water. The membranes were then stored at 4 °C while being immersed in deionized water until membrane modification.

The modification of the BC membrane was based on the optimal conditions determined by Dang et al. [9] which are as follows: 2.44% (w/v) sodium alginate concentration at an impregnation temperature of 30 °C with crosslinking time of 2 hours. The BC membranes were immersed in the indicated sodium alginate concentration for 5 days at a constant temperature of 30 °C. Afterwards, the membranes were crosslinked with 5%(v/v) $CaCl_2$ solution for 2 hours. The modified membranes were then placed in petri dishes and air-dried.

Membrane Characterization

The BCA membranes used in this study were characterized to confirm that they were identical to the optimal membrane determined by Dang et al. [9]. Samples from one batch underwent several tests to determine their properties, thermogravimetric analysis (TGA), Fourier-transform infrared spectroscopy (FTIR), and scanning electron microscopy (SEM) analysis. The hydrophilicity of the membrane was determined by measuring the contact angle through the sessile drop method. The thickness of each membrane used in each experimental run of the FO system was measured as well and taken into consideration when evaluating the results of the process.

Production of Simulated Dirty Water

The feed solution used for this study is simulated dirty water that is based on a study by Roy et al. [19]. Preparation of said solution is modified to fit a laboratory set-up wherein 1 kg of soil is added to 5 L of 0.4 M $CaCl_2$ solution. The resulting solution was left to settle for 3 days then decanted to separate the soil particles from the dirty water produced. The simulated dirty water was then placed in a large plastic container for later use.

Optimization of Forward Osmosis Parameters

The FO experiment was conducted on a laboratory scale FO system, which is illustrated in Figure 1. Polyurethane tubing connects the FS and DS containers to the custom-made membrane module as well as two gear pumps. The flow of FS and DS are recirculated throughout each experimental run which

was conducted for 2 hours with FS and DS having an initial volume of 0.5 L each. Flow rates were set accordingly and kept constant in each experimental run.

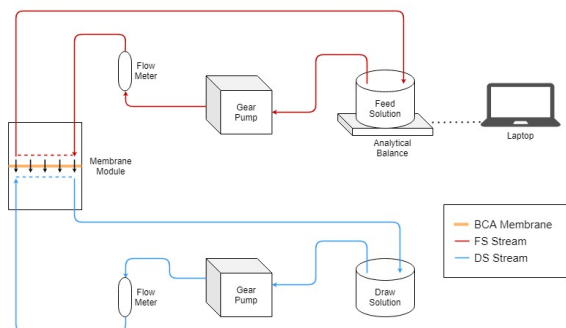


Figure 1 Schematic diagram of forward osmosis system

The performance of a FO process is often evaluated by determining the water flux generated. For the calculation of water flux in this study, the change in mass, operation time, and the known effective area of the membrane were noted following Equation 1. However, the membranes prepared for this study varied in thickness, thus the water flux was normalized to an equal thickness of 1 mm, which is similar to the study of Chrzanowska et al. [23]. The normalized water flux is then calculated using Equation 2 and will be used to evaluate the performance of the process instead.

$$J_w = \frac{\Delta m_{FS}}{\rho_w A_m \Delta t} \quad (1)$$

$$J_{N,i} = J_i \cdot d \quad (2)$$

where J_w is the water flux in $L/m^2 \cdot h$ or LMH, Δm_{FS} is the change in mass of FS in g, ρ_w is the density of water in g/L , A_m is the membrane effective area in m^2 , Δt is the duration of the experimental run in hr, $J_{N,i}$ is the normalized water flux in LMH-mm, J_i is the partial flux in LMH, and d is the thickness of the membrane in mm.

In addition to this, the change in mass of the FS was measured to determine the amount of water recovered by simple arithmetic means. The percentage of water recovered is calculated through Equation 3.

$$\text{Water Recovery} = \frac{m_{F,i} - m_{F,f}}{m_{F,i}} \cdot 100\% \quad (3)$$

where $m_{F,i}$ and $m_{F,f}$ are the initial and final mass of the FS, respectively.

Optimization of the FO process was done through central composite design (CCD) using the software Design Expert 7.0.0. The three factors chosen to be optimized are osmotic pressure, flow rate, and DS to achieve a desirable normalized water flux as the response variable. Experimental runs were designed following face-centered CCD resulting in Table A.3 in the Appendix. Lower and upper limit values, as well as the median of said values, were set for the numerical factors osmotic

pressure and flow rate listed in Table 1. The estimated osmotic pressure of the FS was considered in determining the appropriate values for the osmotic pressure of DS. For flow rate of the FS and DS, the capabilities of the equipment used in the process were taken into account. Meanwhile, DS is a categoric factor consisting of the selected DS for this study which are NaCl, $MgCl_2$, and fructose.

Table 1 Parameters of osmotic pressure and flow rate of draw solutions

Parameters	Lower Limit	Median	Upper Limit
Osmotic Pressure (bar)	40	55	70
Flow Rate (mL/min)	200	250	300

ANOVA was implemented prior optimization to assess the effect of each factor on the response variable and to see if the generated model is appropriate to use in optimizing the three factors. From the solutions provided upon optimization, the optimal operating parameters were chosen based on the practicality of each set of values as well as its desirability, a unitless value ranging from zero to one provided by the software that indicate whether or not the criteria for optimization were met.

3.0 RESULTS AND DISCUSSION

Membrane Selection and Characterization

Out of 110 BCA membranes, the study used the best conditioned ones in terms of even thickness and less deformation. Beforehand, the results of the tests to determine their properties were evaluated in comparison with those used in the study of Dang et al. [9]. The fabricated membranes in this study were found to be much thicker, ranging from 0.3976 to 1.1077 mm, compared to the membranes produced by Dang et al. which ranged from 38.3 μm to 67.6 μm . The membranes were also more hydrophilic, having a lower contact angle with an average value of 10.688° compared to the results of Dang et al. with the range of 28.39° to 32.97°. However, it is worth noting that the sessile drop method was used to measure the contact angle of the membranes. When this method was tested in comparison to the captive bubble method for RO membranes, it showed that the sessile drop method produced inconsistent values despite it commonly being used in numerous studies [24]. Nonetheless, the fabricated membrane in the study is hydrophilic similar to Dang et al. [9].

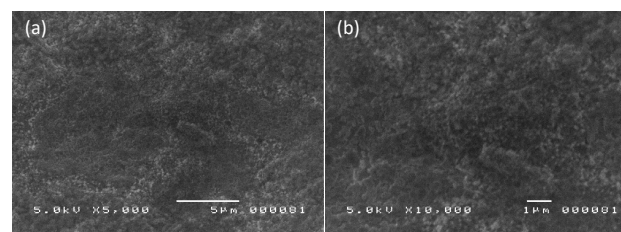


Figure 2 Surface morphology of optimal BCA membrane at magnification of (a) 5,000X and (b) 10,000X

A SEM analysis shown in Figure 2 of the BC membrane prior to modification displayed a dense network of cellulose fibers, similar to the pristine BC membranes produced by Dang et al. as well as to the findings of Suratago et al. [9, 22]. In addition, a TGA

of the BCA membrane showed that its thermal decomposition was initially observed isothermally at around 32 °C with only a small decrease in its weight as shown in Figure 3a. In Figure 3b, its sudden drop in weight is estimated at around 128 °C with a maximum value for its derivative weight change observed to be at 6.9 %/°C. Other studies observed the initial weight loss of their BCA sample to be at 33-150 °C attributing to the loss of water molecules and having a pronounced weight loss at 260-370 °C due to the degradation of BC and sodium alginate [25-26]. However, for the BCA membrane in this study, only minimal changes of the weight were observed within the range of 300 to 800 °C.

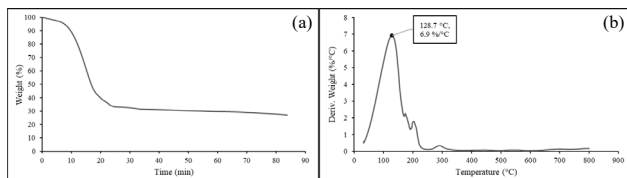


Figure 3 (a) Thermogravimetric analysis data of the BCA membrane and (b) derivative weight change data of the BCA membrane

Results of the FTIR spectrum for the BCA membrane indicated the presence of hydroxyl and carboxyl groups as shown in Figure 4. At a wavenumber of 3372.54 cm^{-1} , a strong absorption band attributed to O-H stretching vibration was observed, similar to the results obtained by Dang et al. and Suratago et al. [9, 22].

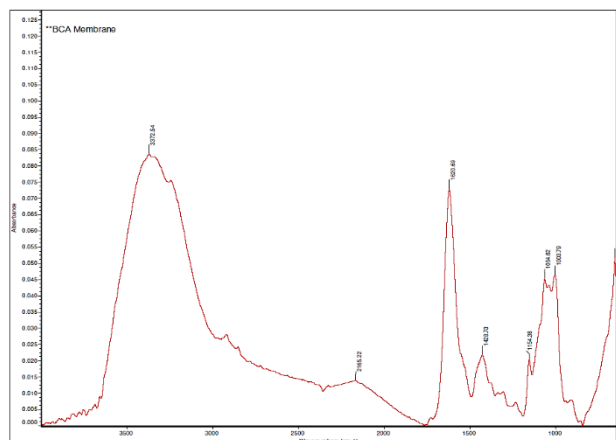


Figure 4 Absorbance of the BCA membrane

Evaluation of Draw Solutions on Forward Osmosis Performance

The effects of osmotic pressure, flow rate, and type of DS were evaluated on the lab-scale FO system using the fabricated BCA membrane with normalized water flux as the response variable. The FS used was simulated dirty water containing 0.4 M CaCl_2 that generated an osmotic pressure around 29 bar. This study did not consider the effect of temperature and was kept constant at room temperature. Since the fabricated BCA membranes varied in thickness, the water flux was normalized to an equal thickness of 1 mm, like that of Chrzanowska et al. using Equation 2 [23]. The three selected DS, NaCl, MgCl_2 , and fructose, were investigated at three flow rates (200, 250, and 300 mL/min) and osmotic pressures of 40, 55, and 70 bar.

Effects of Osmotic Pressure

The results as shown in Figure 5 represent the normalized water flux for each DS at different osmotic pressure and flowrate. Fructose generated a relatively high-water flux ranging from 1.1 to 1.7 LMH·mm at either level of osmotic pressure in comparison with the inorganic salts. However, though not evident, the performance of fructose tends to decrease when osmotic pressure was increased, particularly at low flow rates. The most probable cause for this would be the lowering of driving force at the membrane due to DS dilution. This phenomenon is called dilutive external concentration polarization (ECP) and it is a type of concentration polarization (CP) wherein permeate from the FS enters the draw side and dilutes the DS which in turn lowers the net driving force at the membrane thereby lowering the water flux [27, 24]. Dilutive ECP has been studied to be very significant under system conditions where the FS is non-pure, has a low flowrate, and high water flux [28-30]. There are other types of CP such as internal concentration polarization (ICP), which occurs in the internal structure of the membrane having an active layer and support layer, but since the structure of BCA in this study does not contain those layers, ICP does not apply. Another possibility of the water flux lowering for all solutes could be fouling occurring at the FS side of the membrane. Increasing the osmotic pressure induces higher water flux, but also promotes rapid fouling deposition at the membrane [31-32]. As shown in Figure A.1 in the appendix section, soil and dirt particles were seen deposited at the FS side of the membrane after each run and was observed more evidently at 55 and 70 bar. These particles may have blocked the pores of the membrane and hindered permeate from passing through. Though it may not have affected the flux significantly from the results, this should not be ignored when long-term operation is conducted as fouling increases over time [33].

For NaCl and MgCl_2 (Figure 5a and 5b), both had a positive response and observable trend when osmotic pressure was increased, performing best at 70 bar. A possible reason for this behavior may be due to the salt rejection performance of the membrane preventing reverse solute diffusion (RSD). Increased osmotic pressure means increased DS concentration and water flux, but also increasing the risk of RSD [34]. RSD occurs when ions or molecules from the DS side permeate through the FS side and triggers loss of solute concentration in the DS and fouling at the feed side of the membrane which results to lowering permeate flux [34-35]. However, since the salt selectivity was effective with the BCA membrane, less ions hindered the water from permeating the membrane. The salt rejection for the BCA membrane used in this study was not measured. However, Dang et al. has reported that the BCA membrane had a high salt rejection with a value of 98.36% which is comparable with commercial membranes [9]. Moreover, Suratago et al. also utilized a BCA membrane in the pervaporation of an ethanol-water system, observing that the BCA membrane also exhibited high salt rejection [22].

Effects of Flowrate.

The effect of flowrate was evaluated using an FO system that had a cross-flow design pattern and the flowrate was equally set for both FS and DS. With the trend for each level (200, 250, and 300 mL/min) illustrated in Figure 5, it can be observed that the greatest water flux was obtained at 300 mL/min. Moreover, the effect of increasing the flowrate was more effective on the inorganic solutes than fructose. This is to be expected since it is

generally known that water flux increases at increased cross-flow velocities (CFV) [36]. Due to the turbulent flow of both FS and DS, the effect results to enhanced mixing and levels of concentration difference at the membrane, mitigating ECP [24, 37]. This only affects ECP and not ICP since ECP primarily depends on the change in mass transfer coefficient and the concentration profile in the boundary layer [24]. This is attributed to film theory where, by changing the flow rate, a change in the thickness of the mass transfer boundary layer found at the membrane surface would be observed. At higher flow rates, this boundary layer becomes thinner which result in an acceleration of mass transfer [7, 38].

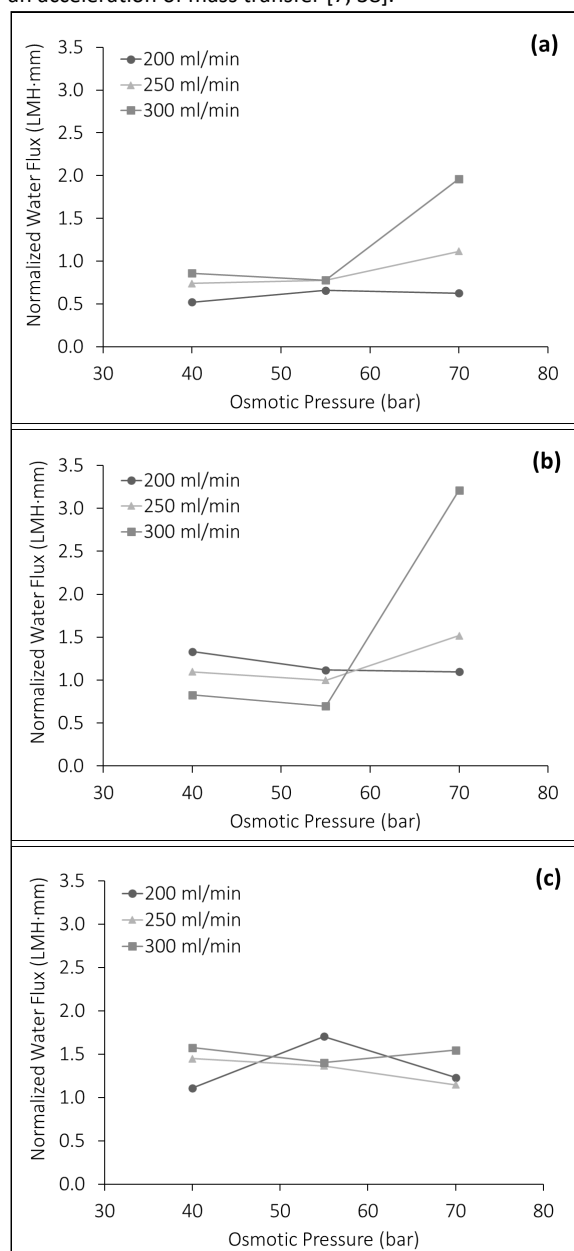


Figure 5 Normalized water flux with respect to osmotic pressure at different flow rates for (a) NaCl, (b) MgCl₂, and (c) Fructose

Suh & Lee [36] observed this from the model that they developed on water flux prediction considering ECP and it showed that at higher CFV, the dilutive ECP decreased from

32.5% to 15.5%. Furthermore, increasing the flowrate also improves removal of foulants due to the high shear stress occurring on the membrane surface allowing for a much thinner and loose fouling layer [6]. This may have also contributed to the improvement of water flux mainly for NaCl and MgCl₂. Similar results have also been observed by Ryu et al. where the increased CFV was able to effectively reduce organic foulants in FO for algae dewatering [20].

Effects of Type of Draw Solution

Aside from flowrate and osmotic pressure, the FO process is easily affected by the properties of the chosen DS, thus careful selection of an appropriate DS could significantly improve its performance. In Figure 6, all solutes exhibited different reactions to the changes in osmotic pressure and flowrate. Fructose showed minimal changes but was able to produce a relatively high flux on either level of set conditions which presents an advantage for an FO process operated at low osmotic pressures and flowrates. Although it must be noted that high concentrations of fructose would not be favorable since the viscosity of the DS would be increased which makes the solution more difficult to pump and would require more energy [39]. This may have been the cause of the slight drop of water flux drawn by fructose at 70 bar despite increasing flowrate. Herron, et al. [40] had similar findings when high fructose corn syrup was used as DS in coffee production and confirmed a linear decrease in flux when DS concentration was increased. Furthermore, it was also observed that high corn fructose syrup had no back diffusion and indicated no significant fouling [40]. Despite the viscosity, the main advantage of simple sugars is their low RSD and non-toxicity which is advantageous for FO applications in the food industry [39].

NaCl had a gradual increase in performance directly proportional to the flowrate and osmotic pressure showing a notable trend at 70 bar. On the other hand, MgCl₂ performed poorly at lower levels of osmotic pressure and declined when flowrate was increased. However, it improved greatly at 70 bar having a similar behavior with NaCl. These findings suggest that both solutes work best at higher osmotic pressures and increased flowrates, but just as mentioned previously, higher osmotic pressure entails a risk of high RSD. Inorganic solutes have been commonly used as DS due to their low-cost and availability but have a disadvantage of showing high RSD even at low DS concentration due to their small molecular size [41]. Monovalent salts such as NaCl show high reverse solute flux (RSF) which have effects of lowering driving force and increased fouling on feed side [8]. Sea salt, mostly comprised of NaCl, was compared with glucose as DS in the study of Ryu, et al. [20] and was found that sea salt exhibited high RSF of 10.4 g/m²/h than glucose with 4.2 g/m²/h. Divalent salts, like MgCl₂, have reduced RSD compared to NaCl due to their larger radii of hydration [13]. This may have been the effect seen in the gathered data where MgCl₂ generated higher water flux than NaCl overall due to their greater electrostatic interaction between the membrane and feed solution which in turn enhanced the salt selectivity. A similar result was observed by Wu et al. [42] when NaCl and MgCl₂ were evaluated using a thin-film composite (TFC) membrane with Milli-Q water as the feed and showed that Mg²⁺ had a lower reverse salt flux than Na⁺ due to enhanced electrostatic interaction.

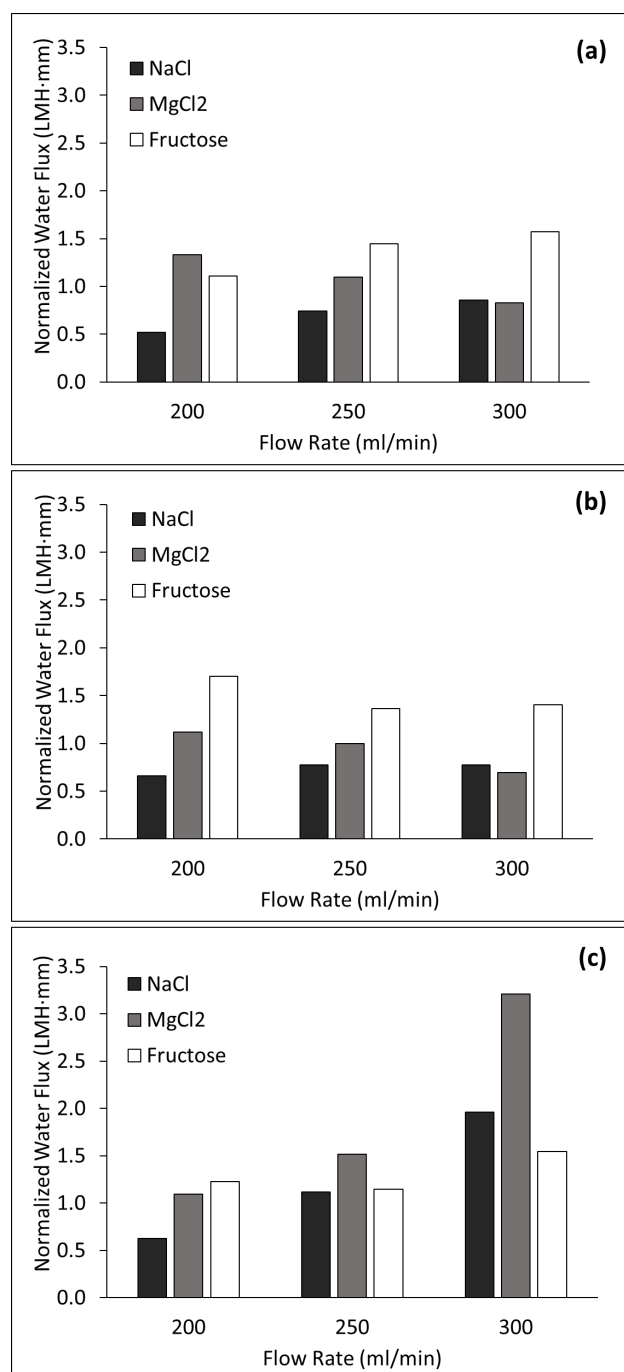


Figure 6 Normalized flux at varying flow rates and draw solution at (a) 40 bar, (b) 55 bar, and (c) 70 bar osmotic pressure

Water Recovery Performance

Low water recovery values were obtained due to the short duration of each run of the FO process which only lasted for 2 hours. However, based on this short duration, fructose had higher water recovery values compared to those of NaCl and MgCl₂. At an osmotic pressure of 70 bar and flow rate of 300 mL/min, the choice of fructose as the DS resulted in a water recovery of 3.11%, the highest value calculated from the gathered data. In comparison, NaCl and MgCl₂ with the same

operating parameters resulted in water recovery values of 1.72% and 2.62%, respectively.

Optimization of Forward Osmosis Operating Parameters

Based on CCD with two numeric factors (osmotic pressure and flow rate), one categorical factor (DS), and one response variable (normalized water flux), a total of 39 experimental runs were conducted following the randomized order set in the software used, Design Expert 7.0.0. Data gathered from the experiment were inputted into the software then analyzed through CCD which resulted to a linear model suggested to be the best fit for the entered data. Initially, the resulting ANOVA table and residual plot showed 2 data points to be significant and were considered outliers. Thus, only 37 out of a total of 39 data points were considered in the optimization of the operating parameters.

Exclusion of the 2 outliers resulted in a better linear model fitting. From the ANOVA table presented in Table A.1, osmotic pressure and flow rate did not have a significant impact on normalized water flux, however DS had a more substantial influence compared to the other 2 factors. With this, optimization of the operating parameters was conducted by first setting the constraints. Normalized water flux was desired to be maximized with its lower and upper limit values obtained from the experimental data. Osmotic pressure and flow rate were also restricted within the range of the lower and upper limits that were set beforehand while DS only included those used in this study.

In Figure 7, a 3D surface response to osmotic pressure and flow rate was constructed for each solution. These responses showed that the normalized water flux has no significant changes with respect to osmotic pressure and flow rate, as found from the results of Table A.1, however the DS itself has a significant effect on the resulting normalized water flux. The 3D surface response for fructose shows the highest predicted range of normalized flux from about 1.35 to 1.45 LMH·mm as seen in Figure 7c. Its range of predicted values is of greater value compared to that of NaCl and MgCl₂ which are estimated to be in the range of 0.75 to 0.85 LMH·mm and 1.0 to 1.2 LMH·mm, respectively.

Table 2 Solutions for Three Combinations of Categorical Factor Levels

Solution	Osmotic Pressure (bar)	Flow Rate (ml/min)	Draw Solution	Normalized Water Flux (LMH·mm)	Desirability
1	70.0	300.0	Fructose	1.437	0.768
2	70.0	300.0	MgCl ₂	1.129	0.510
3	70.0	300.0	NaCl	0.826	0.257
4	69.7	300.0	NaCl	0.825	0.256

In addition, four solutions were provided by the software for the optimization of the collected data, shown in Table 2, with the solution having a high desirability of 0.768 deemed as the optimal choice. Therefore, the optimal operating parameters resulted with fructose as the DS and the osmotic pressure and flow rate set to 70 bar and 300 mL/min, respectively. A

normalized water flux of 1.437 LMH-mm is predicted given the optimal values for the factors.

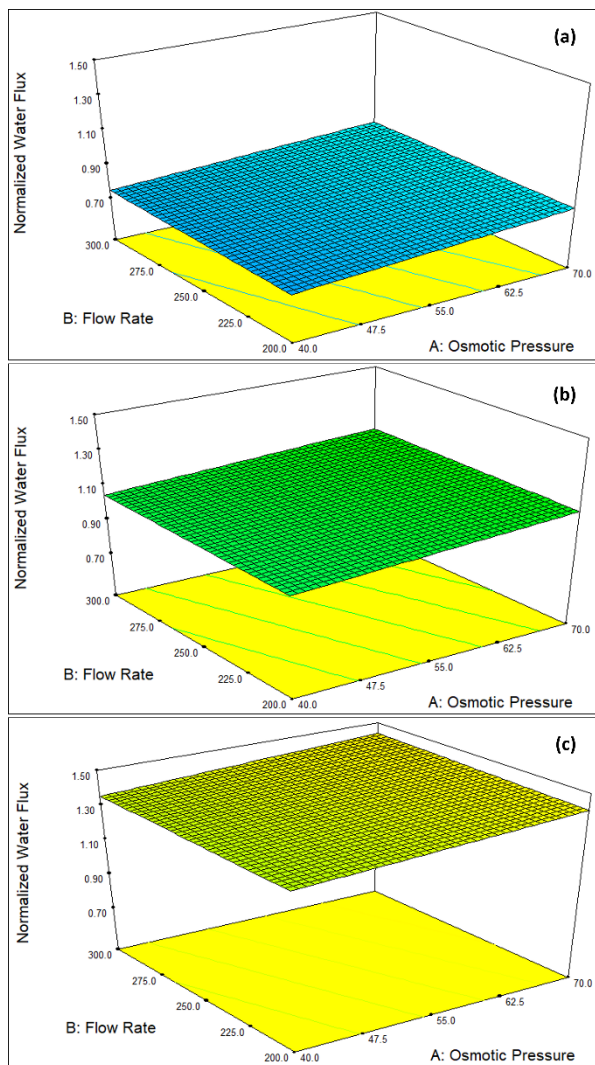


Figure 7 Normalized water flux 3D surface response to flow rate and osmotic pressure for (a) NaCl, (b) MgCl₂, and (c) fructose

4.0 CONCLUSION

The FO performance using the optimal BCA membrane was evaluated by considering three factors: osmotic pressure, flow rate, and type of DS. Osmotic pressure and flow rate did not have a substantial influence on the normalized water flux, however the type of DS, and in turn their properties, significantly affected the performance of the process. Optimization through CCD resulted in four solutions among which fructose at an osmotic pressure of 70 bar and flow rate of 300 mL/min were deemed as the optimal operating conditions when using BCA membrane for the FO process. With these optimal conditions, the normalized water flux is predicted to be 1.437 LMH-mm. To further examine the validity of this result, a confirmation run and duplication of this experiment are recommended for future studies who plan to further investigate and improve upon the results of this study.

Acknowledgement

The authors would like to acknowledge Engr. Jesuñino Aquino of the Chemical Engineering Department, Malayan Colleges Laguna for his assistance in the FO experiments.

References

- [1] Almaden, C. R. 2014. Protecting the Water Supply: The Philippine Experience. *Journal of Social, Political and Economic Studies*. 39(4): 467-493. Online: <https://ssrn.com/abstract=2542792>
- [2] Asian Development Bank. 2016. Asian Water Development Outlook 2016: Strengthening Water Security in Asia and the Pacific. Online: <https://www.adb.org/publications/asian-water-development-outlook-2016>
- [3] Asian Development Bank. 2020. Asian Water Development Outlook 2020: Advancing Water Security across Asia and the Pacific. Online: <https://www.adb.org/sites/default/files/publication/663931/awdo-2020.pdf>
- [4] Elimelech, M and Phillip, W. A. 2011. The Future of Seawater Desalination: Energy, Technology, and the Environment. *Science*. 333(6043): 712-717. DOI: <https://doi.org/10.1126/science.1200488>
- [5] Suwaileh, W., Pathak, N., Shon, H., and Hilal, N. 2020. Forward Osmosis Membranes and Processes: A Comprehensive Review of Research Trends and Future Outlook. *Desalination*. 485(114455). DOI: <https://doi.org/10.1016/j.desal.2020.114455>
- [6] Lee, S., Boo, C., Elimelech, M., and Hong, S. 2010. Comparison of Fouling Behavior in Forward Osmosis (FO) and Reverse Osmosis (RO). *Journal of Membrane Science*. 365(1-2): 34-39. DOI: <https://doi.org/10.1016/j.memsci.2010.08.036>
- [7] Xu, W., Chen, Q., and Ge, Q. 2017. Recent Advances in Forward Osmosis (FO) Membrane: Chemical Modifications on Membranes for FO Processes. *Desalination*. 419: 101-116. DOI: <https://doi.org/10.1016/j.desal.2017.06.007>
- [8] Akther, N., Sodiq, A., Giwa, A., Daer, S., Arafat, H. A., and Hasan, S. W. 2015. Recent Advancements in Forward Osmosis Desalination: A Review. *Chemical Engineering Journal*. 281: 502-522. DOI: <https://doi.org/10.1016/j.cej.2015.05.080>
- [9] Dang, N. T. B., Patacsil, L. B., Orbecido, A. H, Eusebio, R. C., and Beltran, A. B. 2018. Evaluation of Bacterial Cellulose-Sodium Alginate Forward Osmosis Membrane for Water Recovery. *Jurnal Teknologi*. 80 (3-2): 37-43. DOI: <https://doi.org/10.11113/jt.v80.12742>
- [10] Esa, F., Tasirin, S. M., and Rahman, N. A. 2014. Overview of Bacterial Cellulose Production and Application. *Agriculture and Agricultural Science Procedia*. 2: 113-119. DOI: <https://doi.org/10.1016/j.aaspro.2014.11.017>
- [11] Bautista-Patacsil, L., Ligaray, M. V., Sayao, J. P., Belosillo, J. R., Eusebio, R. C., Orbecido, A. H., and Beltran, A. B. 2020. Fabrication of Forward Osmosis Membrane Using Nata de Coco as Raw Materials for Desalination. *Taiwan Water Conservancy*. 68(1): 36-43. DOI: [https://doi.org/10.6937/TWC.202003/PP_68\(1\).0004](https://doi.org/10.6937/TWC.202003/PP_68(1).0004)
- [12] Alberto, E. L., de Ocampo, A. N., Depasupil, C. G., Ligaray, M., Eusebio, R. C., Orbecido, A. H., Beltran, A. B., and Patacsil, L. B. 2019. Desalination Performance of a Forward Osmosis Membrane from Acetylated Nata de Coco (Bacterial Cellulose). *AIP Conference Proceedings*. 2124(1). DOI: <https://doi.org/10.1063/1.5117085>
- [13] Achilli, A., Cath, T. Y., and Childress, A. E. 2010. Selection of Inorganic-Based Draw Solutions for Forward Osmosis Applications. *Journal of Membrane Science*. 364(1-2): 233-241. DOI: <https://doi.org/10.1016/j.memsci.2010.08.010>
- [14] Ge, Q., Ling, M., and Chung, T. S. 2013. Draw Solutions for Forward Osmosis Processes: Developments, Challenges, and Prospects for the Future. *Journal of Membrane Science*. 442: 225-237. DOI: <https://doi.org/10.1016/j.memsci.2013.03.046>
- [15] Luo, H., Wang, Q., Zhang, T. C., Tao, T., Zhou, A., Chen, L., and Bie, X. 2014. A Review on the Recovery Methods of Draw Solutes in Forward Osmosis. *Journal of Water Process Engineering*. 4: 212-223. DOI: <https://doi.org/10.1016/j.jwpe.2014.10.006>
- [16] Holloway, R. W., Maltos, R., Vanneste, J., and Cath, T. Y. 2015. Mixed Draw Solutions for Improved Forward Osmosis Performance. *Journal of Membrane Science*. 491: 121-131. DOI: <https://doi.org/10.1016/j.memsci.2015.05.016>

- [17] Dou, P., Zhao, S., Song, J., He, H., She, Q., Li, X., Zhang, Y., and He, T. 2019. Forward Osmosis Concentration of a Vanadium Leaching Solution. *Journal of Membrane Science*. 582: 164-171. DOI: <https://doi.org/10.1016/j.memsci.2019.04.012>
- [18] Bowden, K. S., Achilli, A., and Childress, A. E. 2012. Organic Ionic Salt Draw Solutions for Osmotic Membrane Bioreactors. *Bioresource Technology*. 122: 207-216. DOI: <https://doi.org/10.1016/j.biortech.2012.06.026>
- [19] Roy, D., Rahni, M., Pierre, P., and Yargeau, V. 2016. Forward Osmosis for the Concentration and Reuse of Process Saline Wastewater. *Chemical Engineering Journal*. 287: 277-284. DOI: <https://doi.org/10.1016/j.cej.2015.11.012>
- [20] Ryu, H., Kim, K., Cho, H., Park, E., Chang, Y. K., and Han, J. 2020. Nutrient-driven Forward Osmosis Coupled with Microalgae Cultivation for Energy Efficient Dewatering of Microalgae. *Algal Research*. 48: 101880. DOI: <https://doi.org/10.1016/j.algal.2020.101880>
- [21] Rodriguex-Saona, L. E., Giusti, M. M., Durst, R. W., and Wrolstad, R. E. 2001. Development and Process Optimization of Red Radish Concentrate Extract as Potential Natural Red Colorant. *Journal of Food Processing and Preservation*. 25(3):165-182. DOI: <https://doi.org/10.1111/j.1745-4549.2001.tb00452.x>
- [22] Suratago, T., Taokaew, S., Kanjanamosit, N., Kanjanaprapakul, K., Burapatana, V., and Phisalaphong, M. 2015. Development of Bacterial Cellulose/Alginate Nanocomposite Membrane for Separation of Ethanol-Water Mixtures. *Journal of Industrial and Engineering Chemistry*. 32: 305-312. DOI: <https://doi.org/10.1016/j.jiec.2015.09.004>
- [23] Chrzanowska, E., Gierszewska, M., Kujawa, J., Raszowska-Kaczor, A., and Kujawski, W. 2018. Development and Characterization of Polyamide-supported Chitosan Nanocomposite Membranes for Hydrophilic Pervaporation. *Polymers*. 10(8). DOI: <https://doi.org/10.3390/polym10080868>
- [24] Bhinder, A., Shabani, S., and Sadrzadeh, M. 2017. Effect of Internal and External Concentration Polarizations on the Performance of Forward Osmosis Process. In *Osmotically Driven Membrane Processes - Approach, Development and Current Status*, Du, H., Thompson, A., and Wang, X. (Eds.), [Online]. DOI: <https://doi.org/10.5772/intechopen.71343>
- [25] Shao, W., Liu, H., Liu, X., Wang, S., Wu, J., Zhang, R., ... and Huang, M. 2015. Development of Silver Sulfadiazine Loaded Bacterial Cellulose/Sodium Alginate Composite Films with Enhanced Antibacterial Property. *Carbohydrate Polymers*. 132: 351-358. DOI: <https://doi.org/10.1016/j.carbpol.2015.06.057>
- [26] Bai, Q., Xiong, Q., Li, C., Shen, Y., and Uyama, H. 2018. Hierarchical Porous Carbons from a Sodium Alginate / Bacterial Cellulose Composite for High-Performance Supercapacitor Electrodes. *Applied Surface Science*. 455: 795-807. DOI: <https://doi.org/10.1016/j.apsusc.2018.05.006>
- [27] McCutcheon, J. R. and Elimelech, M. 2006. Influence of Concentrative and Dilutive Internal Concentration Polarization on Flux Behavior in Forward Osmosis. *Journal of Membrane Science*. 284(1-2): 237-247. DOI: <https://doi.org/10.1016/j.memsci.2006.07.049>
- [28] Gruber, S. M. F., Johnson, C. J., Tang, C. Y., Jensen, M. H., Yde, L., and Hélix-Nielsen, C. 2011. Computational Fluid Dynamics Simulations of Flow and Concentration Polarization in Forward Osmosis Membrane Systems. *Journal of Membrane Science*. 379(1-2): 488-495. DOI: <https://doi.org/10.1016/j.memsci.2011.06.022>
- [29] Sagiv, A. and Semiat, R. 2011. Finite Element Analysis of Forward Osmosis Process using NaCl Solutions. *Journal of Membrane Science*. 379(1-2): 86-96. DOI: <https://doi.org/10.1016/j.memsci.2011.05.042>
- [30] McCutcheon, J. R. and Elimelech, M. 2007. Modeling Water Flux in Forward Osmosis: Implications for Improved Membrane Design. *AIChE Journal*. 53(7): 1736-1744. DOI: <https://doi.org/10.1002/aic.11197>
- [31] Phuntsho, S., Sahebi, S., Majeed, T., Lofti, F., Kim, J., and Shon, H. 2013. Assessing the Major Factors Affecting the Performances of Forward Osmosis and Its Implications on the Desalination Process. *Chemical Engineering Journal*. 231: 484-496. DOI: <https://doi.org/10.1016/j.cej.2013.07.058>
- [32] Wenten, I. G., Khoiruddin, K., Reynard, R., Lugito, G., and Julian, H. 2020. Advancement of Forward Osmosis (FO) Membrane for Fruit Juice Concentration. *Journal of Food Engineering*. 290: 110216 DOI: <https://doi.org/10.1016/j.jfoodeng.2020.110216>
- [33] Chun, Y., Mulcahy, D., Zou, L., and Kim, I. 2017. A Short Review of Membrane Fouling in Forward Osmosis Processes. *Membranes*. 7(2). DOI: <https://doi.org/10.3390/membranes7020030>
- [34] Tang, C. Y., She, Q., Lay, W. C. L., Wang, R., and Fane, A. G. 2010. Coupled Effects of Internal Concentration Polarization and Fouling On Flux Behavior of Forward Osmosis Membranes During Humic Acid Filtration. *Journal of Membrane Science*. 354(1-2): 123-133. DOI: <https://doi.org/10.1016/j.memsci.2010.02.059>
- [35] She, Q., Wang, R., Fane, A. G., and Tang, C. Y. 2016. Membrane Fouling in Osmotically Driven Membrane Processes: A Review. *Journal of Membrane Science*. 499: 201-233. DOI: <https://doi.org/10.1016/j.memsci.2015.10.040>
- [36] Suh, C. and Lee, S. 2013. Modeling Reverse Draw Solute Flux in Forward Osmosis with External Concentration Polarization in Both Sides of the Draw and Feed Solution. *Journal of Membrane Science*. 427: 365-374. DOI: <https://doi.org/10.1016/j.memsci.2012.08.033>
- [37] Abid, H. S., Johnson, D. J., Hashaikheh, R., and Hilal, N. 2017. A Review of Efforts to Reduce Membrane Fouling by Control of Feed Spacer Characteristics. *Desalination*. 420: 384-402. DOI: <https://doi.org/10.1016/j.desal.2017.07.019>
- [38] Wong, M., Martinez, K., Ramon, G. Z., and Hoek, E. 2012. Impacts of Operating Conditions and Solution Chemistry on Osmotic Membrane Structure and Performance. *Desalination*. 287: 340-349. DOI: <https://doi.org/10.1016/j.desal.2011.10.013>
- [39] Terefe, N. S., Janakievski, F., Glagovskaia, O., and Stockmann, R. 2019. Forward Osmosis: An Emerging Non-Thermal Concentration Technology for Liquid Foods. In *Reference Module in Food Science*, [Online]. DOI: <https://doi.org/10.1016/B978-0-08-100596-5.21871-4>
- [40] Herron, J., Beaudry, E. G., Jochums, C. E., and Medina, L. E. 1994. Osmotic Concentration Apparatus for Direct Osmotic Concentration of Fruit Juices. USA Patent Application 986921.
- [41] Johnson, D. J., Suwaileh, W. A., Mohammed, A. W., and Hilal, N. 2018. Osmotic's Potential: An Overview of Draw Solutes for Forward Osmosis. *Desalination*. 434: 100-120. DOI: <https://doi.org/10.1016/j.desal.2017.09.017>
- [42] Wu, C., Mouri, H., Chen, S., Zhang, D., Koga, M., and Kobayashi, J. 2016. Removal of Trace-amount Mercury from Wastewater by Forward Osmosis. *Journal of Water Process Engineering*. 14: 108-116. DOI: <https://doi.org/10.1016/j.jwpe.2016.10.010>

Appendix

Table A.1 Final ANOVA table of the linear model for normalized water flux

Source	Sum of Squares	df	Mean Square	F Value	p-value Prob>F	
Model	2.39	4	0.60	10.34	<0.0001	significant
A: Osmotic Pressure	0.025	1	0.025	0.44	0.5119	
B: Flow Rate	0.002984	1	0.002984	0.052	0.8217	
C: Draw Solution	2.31	2	1.16	20.01	<0.0001	
Residual	1.85	32	0.058			
Lack of Fit	1.00	20	0.050	0.71	0.7623	not significant
Pure Error	0.85	12	0.071			
Total	4.24	36				

Table A.2 Corresponding Concentrations of the Draw Solutions

Draw Solution	Concentration (M)		
	Lower Limit	Median	Upper Limit
NaCl	0.8	1.1	1.4
MgCl ₂	0.5	0.7	0.9
Fructose	1.6	2.2	2.8

Table A.3 Design of Experiment for Optimization

Standard Order	Run Order	Factor 1 A: Osmotic Pressure (bar)	Factor 2 B: Flow Rate (mL/min)	Factor 3 C: Draw Solution
15	1	70.0	200	MgCl ₂
39	2	55.0	250	Fructose
36	3	55.0	250	Fructose
18	4	40.0	250	MgCl ₂
32	5	70.0	250	Fructose
8	6	55.0	300	NaCl
26	7	55.0	250	MgCl ₂
12	8	55.0	250	NaCl
5	9	40.0	250	NaCl
10	10	55.0	250	NaCl
31	11	40.0	250	Fructose
14	12	40.0	200	MgCl ₂
33	13	55.0	200	Fructose
20	14	55.0	200	MgCl ₂
1	15	40.0	200	NaCl
2	16	70.0	200	NaCl
27	17	40.0	200	Fructose
38	18	55.0	250	Fructose
7	19	55.0	200	NaCl
3	20	40.0	300	NaCl
21	21	55.0	300	MgCl ₂
11	22	55.0	250	NaCl
30	23	70.0	300	Fructose
37	24	55.0	250	Fructose
6	25	70.0	250	NaCl
24	26	55.0	250	MgCl ₂
16	27	40.0	300	MgCl ₂
23	28	55.0	250	MgCl ₂
19	29	70.0	250	MgCl ₂
4	30	70.0	300	NaCl
13	31	55.0	250	NaCl
25	32	55.0	250	MgCl ₂
29	33	40.0	300	Fructose
9	34	55.0	250	NaCl
28	35	70.0	200	Fructose
22	36	55.0	250	MgCl ₂
17	37	70.0	300	MgCl ₂
35	38	55.0	250	Fructose
34	39	55.0	300	Fructose

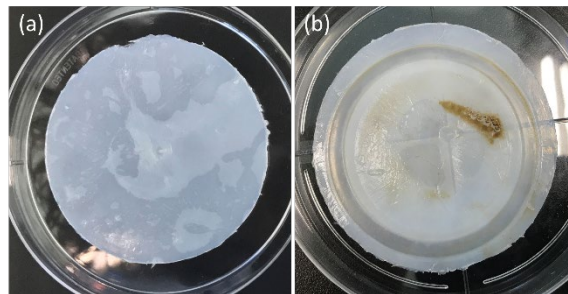


Figure A.1 BCA membrane (a) before and (b) after the FO proces